

Guidelines to Set CST Solver Accuracy and Mesh Parameter Settings to Improve Simulation Results with the Time Domain Solver and Hexahedral Meshing System illustrated with a finite length horizontal dipole over a ground plane

CST Simulation Study, Part 2

Tom Mozdzen

11/11/2014

Choosing the correct mesh parameters is vital to getting accurate CST simulation results. The purpose of this memo is to give users the knowledge to quickly set up a simulation and be confident of the results. A finite length horizontal dipole was used to study the meshing and accuracy settings. More specific dipole results are described in the second section of this report. In summary, it was found that 35 of the 38 mesh settings investigated gave similarly good results, while only 3 settings gave poor results. Seven of the good settings were better than average. The metric judging the results will be described in section 2.

I. Meshing and Accuracy Settings

Mesh Basics

CST provides four meshing modes. For simplicity, start with the PBA mode and later move to the EFPBA mode if the mesh density becomes very high (> 100 lines per wavelength). Although PBA and EFPBA seem to give similar results as seen by Figure 1, the mesh generator will fail when the density of mesh cells becomes too high and will suggest using EFPBA. Increasing the mesh lines per wavelength increases the mesh cell count and simulation time, so the goal is to get the desired accuracy without overkill on mesh cell count. Sometimes excessive mesh counts can actually lead to less accurate simulation results. Here is a list of the four mesh styles and Figure 1 shows a benchmark study done by the CST developers.

- Staircase
- FPBA - Fast Perfect Boundary Approximation
- PBA - Perfect Boundary Approximation
- EFPBA - Enhanced Accuracy FPBA

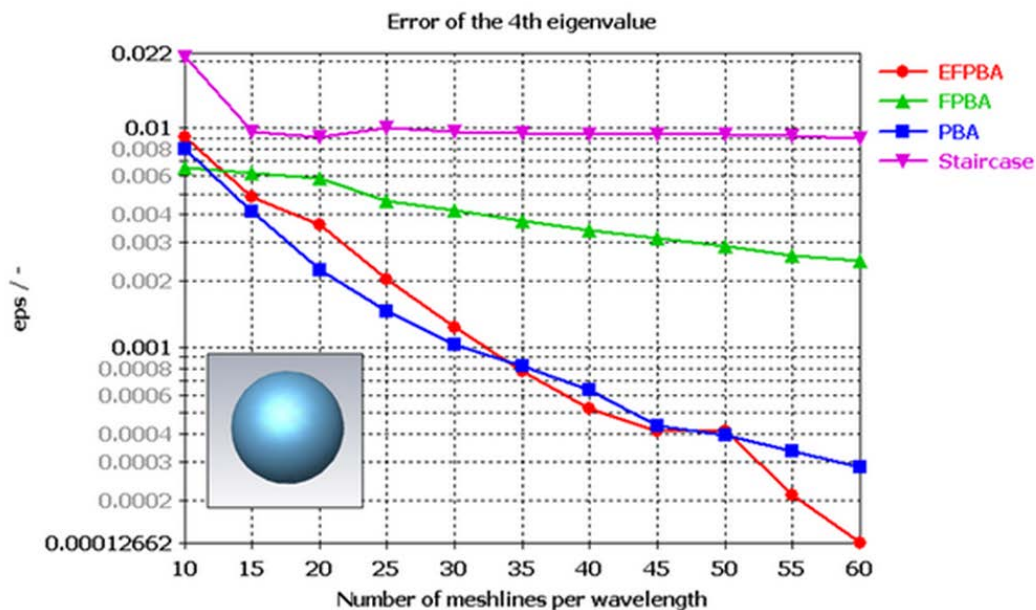


Figure 1. CST's internal benchmark of the four meshing schemes.

Mesh Refinements

The mesh is determined by four sets of menus: The Solver Menu, the Mesh Global Properties Menu, the Boundaries Menu, and the Background Settings Menu.

The Solver Menu

Adaptive Mesh Refinement – via the Solver Menu (plus two solver settings to note)

It is best to enable adaptive meshing in the beginning to get a rough estimate for the mesh density that is needed to generate stable results. The shape of the S11 curve will stabilize when the mesh density reaches a critical level. The beam shape is also affected by the mesh.

Solver Settings

Set the Accuracy value to -80, this is as high as it will go. Under the “Specials...” settings, the first special tab will let you set the number of pulses. CST support recommends to up this number to 50.

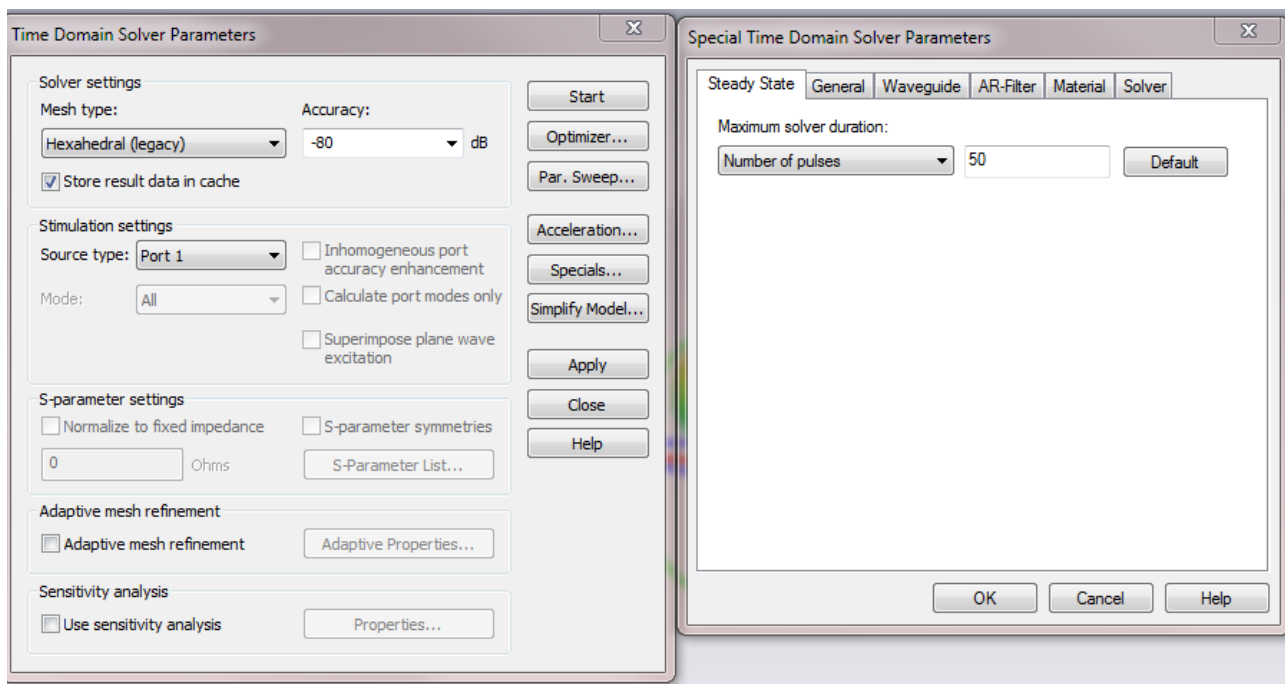


Figure 2. Solver settings for Accuracy = -80 dB and Number of pulses = 50.

Adaptive Mesh Settings

Figure 3 shows the dialog screen for adaptive mesh settings. The Energy based method is more flexible in that it will work with sub-gridding (explained next), while the Expert System based will not. Choose the minimum and maximum number of passes as well as the frequency range for the checks and the maximum delta between runs which is used for a stop criteria. "Number of checks" means how many successive runs of meeting the max delta criteria are required for a stop. The refinement settings at the bottom can also be adjusted.

It was found that the best mesh was found early on, and that denser meshes did not always lead to better solutions. This is something the user has to experiment with.

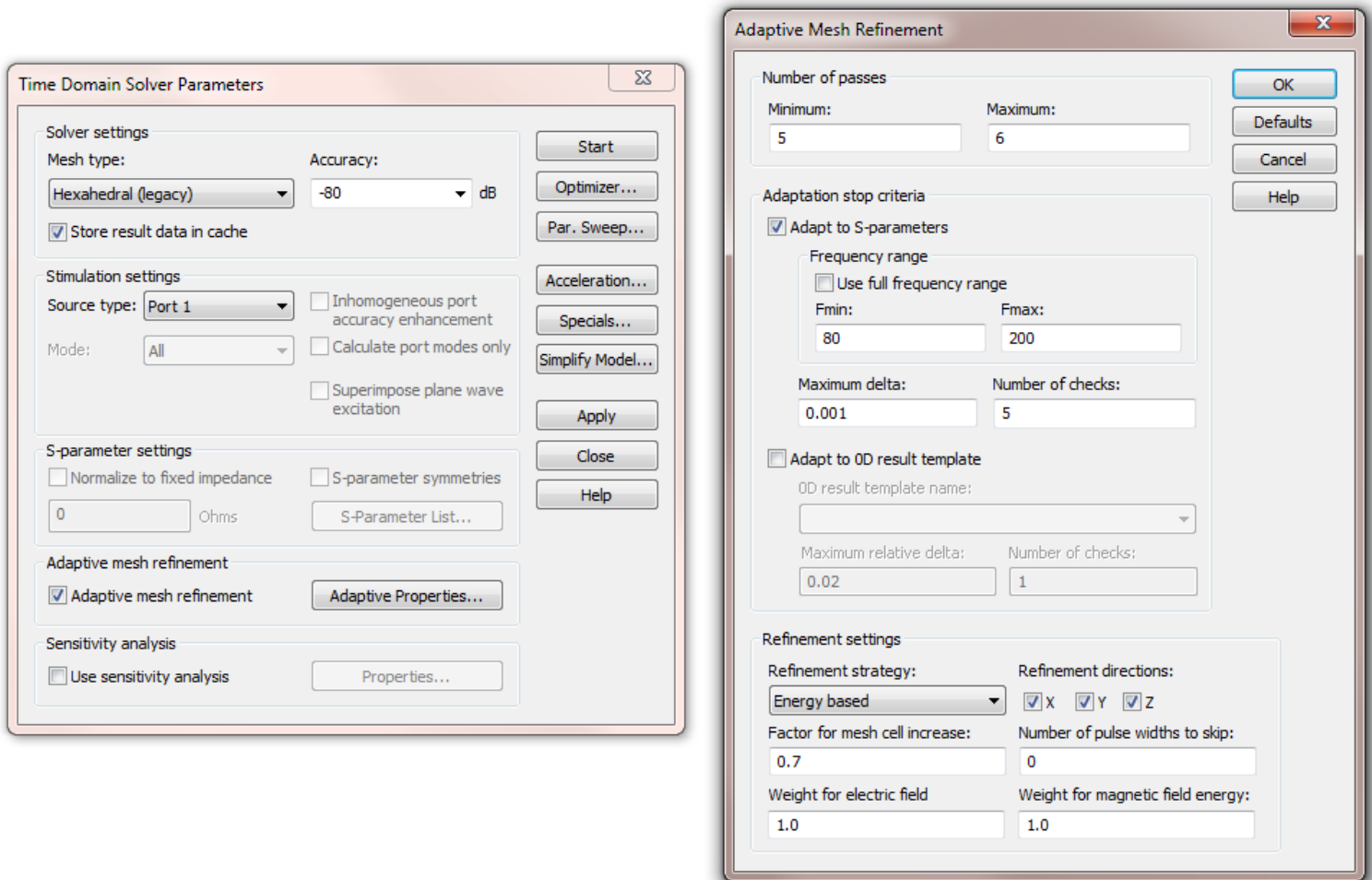


Figure 3. Solver Settings Menu to select Adaptive mesh refinement and its properties.

Result Storage Locations

Adaptive meshing will run complete simulations and store them in the results cache and will stop when changes to the S11 curve are below the specified threshold and the minimum number of passes has been reached. The directory system is shown in Figure 4. Warning: Do not re-simulate any re-opened cache .cst file as the results will corrupt the directory structure which will prevent subsequent simulations from saving results. You will have to copy the original file at the top level to another name and run fresh simulations to continue.

If you want to re-simulate a cached solution, copy that file to a top level directory with a different name, without the accompanying folder, and use that as a starting point for a new simulation.

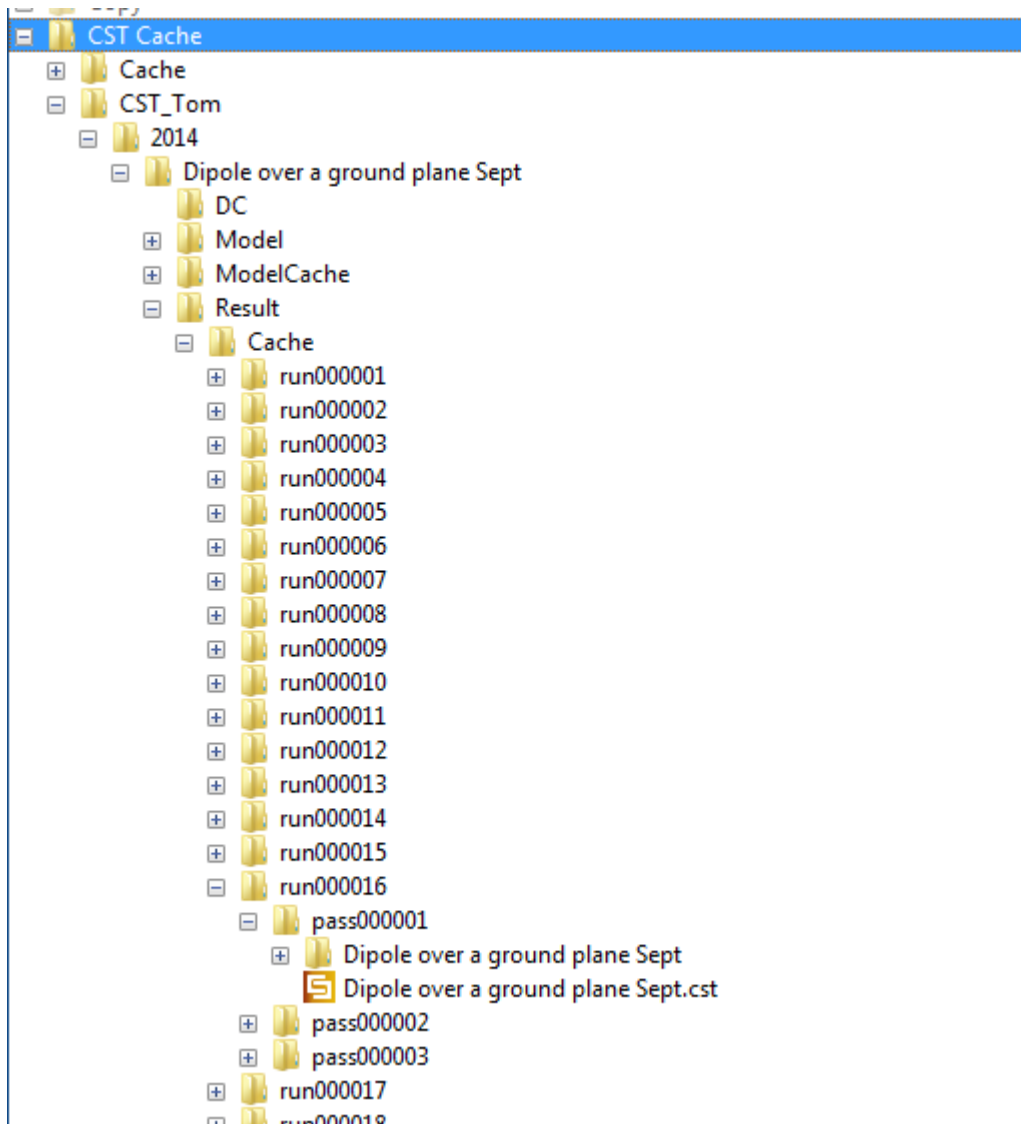


Figure 4. Stored results are in the Results Cache for multiple runs. The runs are generated by either parameter sweeps, adaptive mesh runs (with pass00000x subdirectories), or new model settings. Open the file of interest to see full results, but do not re-simulate a file in the Results Cache as this will corrupt your main directory and no further results will be able to be saved again.

The Mesh Global Properties Menu

Sub-gridding – via the Global Mesh Properties Menu (MSS – Multilevel Sub-gridding System)

The global mesh properties menu has many variables which can be modified. One of these variables is whether to use sub-gridding or not. When sub-gridding is not used, the finest mesh dimensions are extended all the way across the simulation boundary. When sub-gridding is enabled, the fine mesh steps are only enabled near the points of interest and decrease further away from the structure which caused the mesh to become dense. Figure 5 illustrates this. CST recommends not to use sub-gridding unless the number of mesh cells is reduced by a factor of 3 as sub-gridding requires extra overhead and will slow the simulation down. However, I've found that by not using sub-gridding, the number of mesh cells can grow too quickly and actually lead to less accurate results.

The Equilibrate mesh ratio and max cell aspect ratio affect how much larger a mesh cell can be as compared to its neighbor. The refine at metal edges factor is also a parameter that can adjust local mesh values. I did not see a significant change in the simulation results when these parameters were modified.

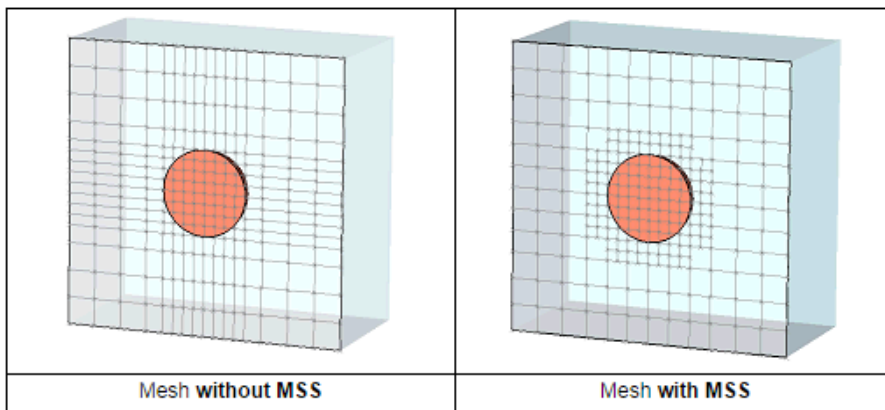
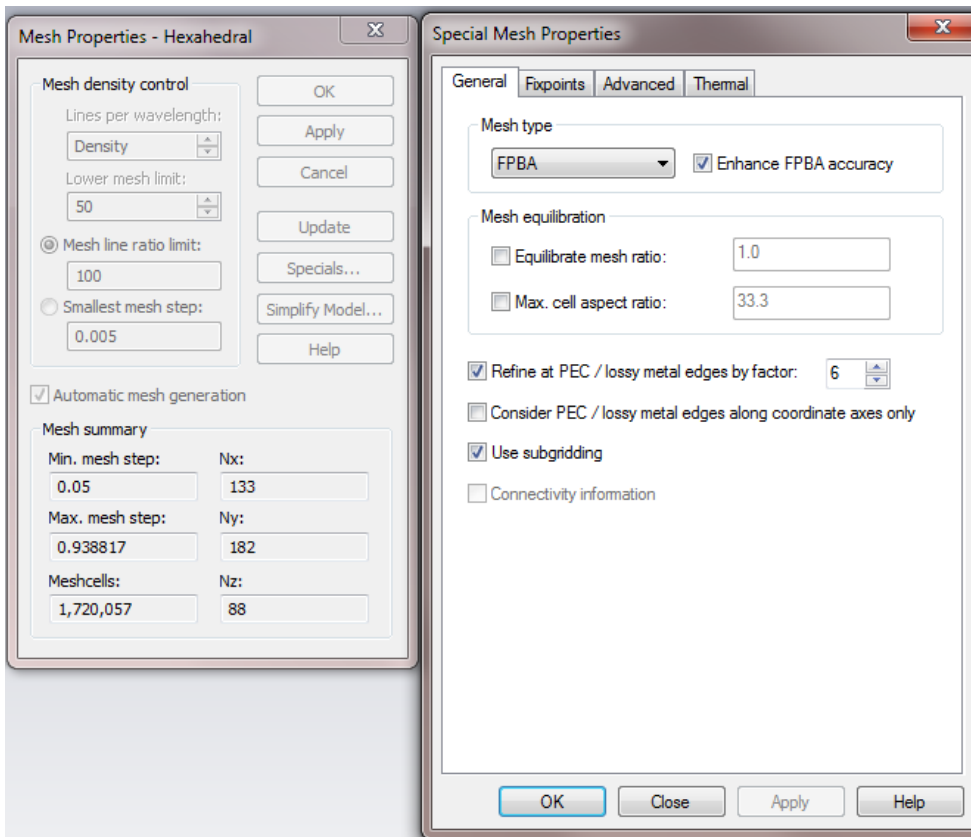


Figure 5. Illustration of the mesh with and without sub-gridding turned on.

The Fix Points Tab and the Advanced Tab.

No settings were adjusted on the Fixpoints tab, but all boxes should be checked (default). On the Advanced tab, the “point accuracy enhancement value was generally modified to a higher value of 75 to 95 %, but again, no significant trends were noticed. The “Use TST cells” should be checked by default. The Thermal Tab settings are not used.

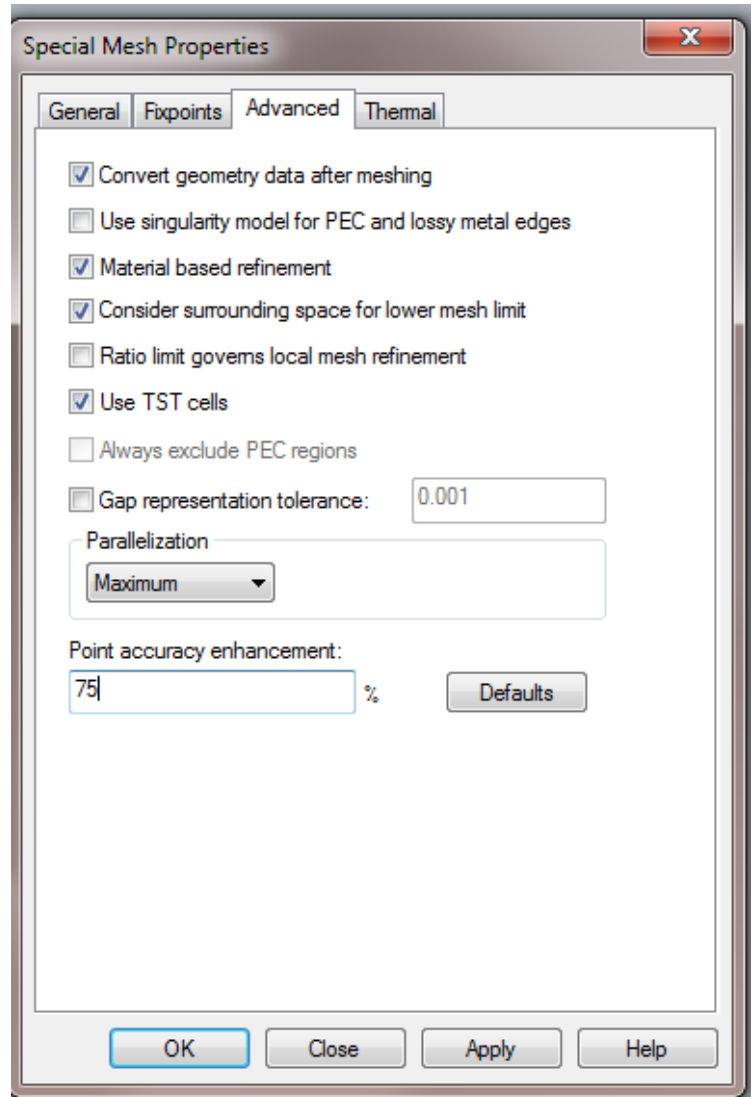
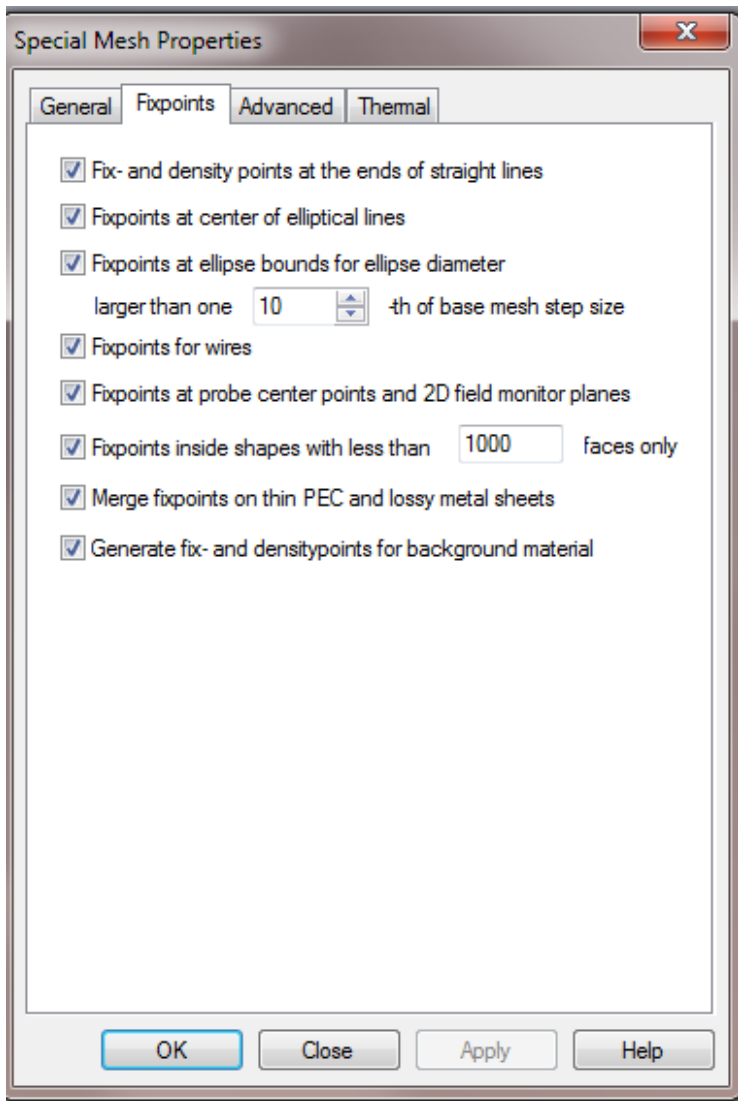


Figure 6. Special Mesh Properties tabs Fixpoints and Advanced. Everything on the Fixpoints tab should be checked and the TST box of the Advanced Tab should be checked as well as the Point accuracy enhancement boosted from 0% to 75-95%.

The Bounding Box Menu and the Background Menu

These menus can be found on the “Settings” section at the far left hand side of the ribbon in the main Simulation tab. The bounding box settings has a significant effect upon the simulation results. Figure 7 shows the bounding box view when the Bounding Box menu is selected. Along with the “Open Boundary” dialog.

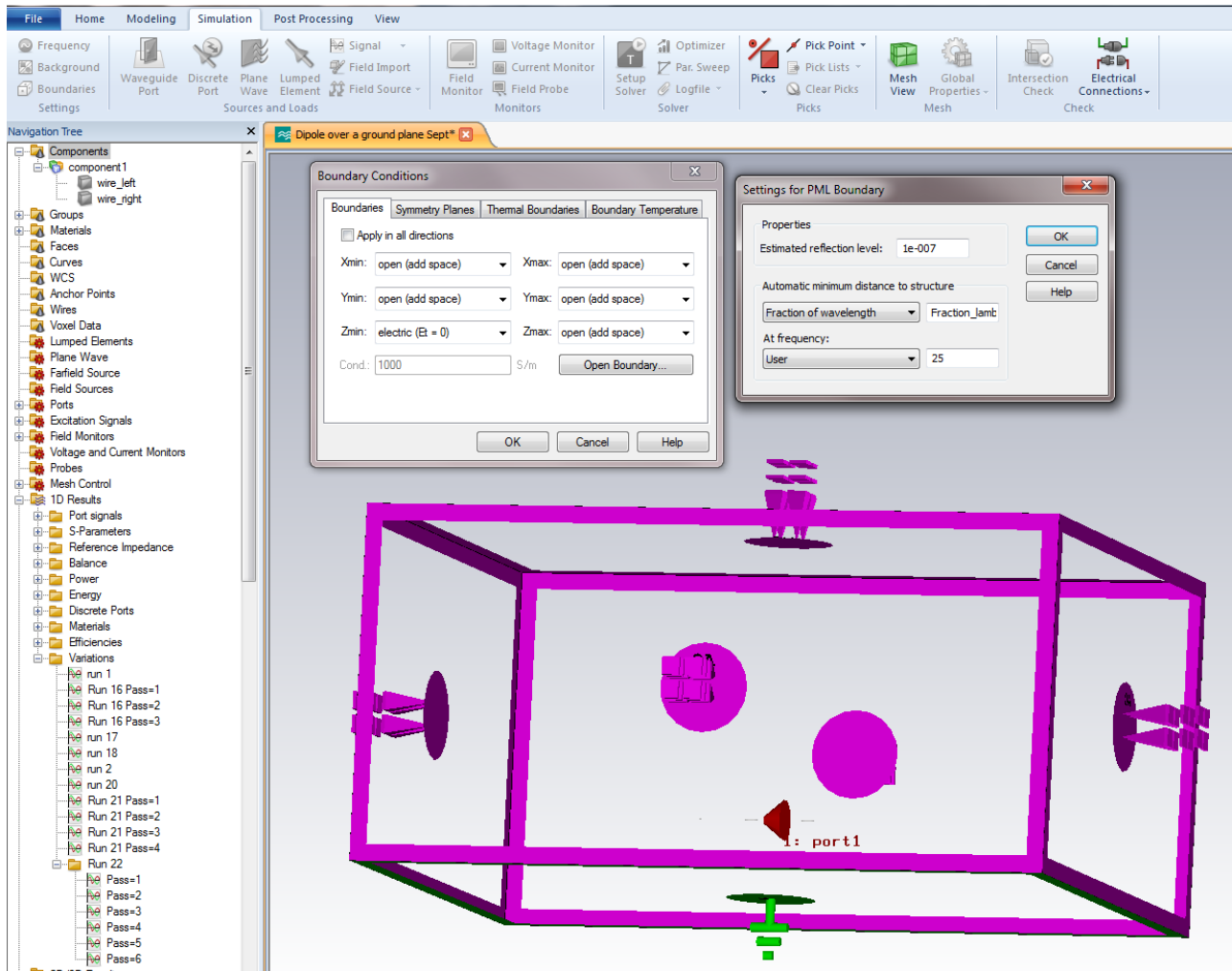


Figure 7. Bounding box settings.

By default, the simulator adds 1/8 of a wavelength between the structure and the edge of the simulation space. That fraction can be increased up to a full wavelength at the frequency specified by the user. 50 MHz (not 25 MHz as shown) was the typical frequency used for the better yielding results. See Figure 9.

One can also add more space by opening the “Background” settings menu (see Fig. 10). However, the default setting of 1/8 wavelength appears to give the most reproducible results. Adding more space increases the number of mesh cells, but does not improve the beam pattern as measured by the finite length horizontal dipole over a ground plane.

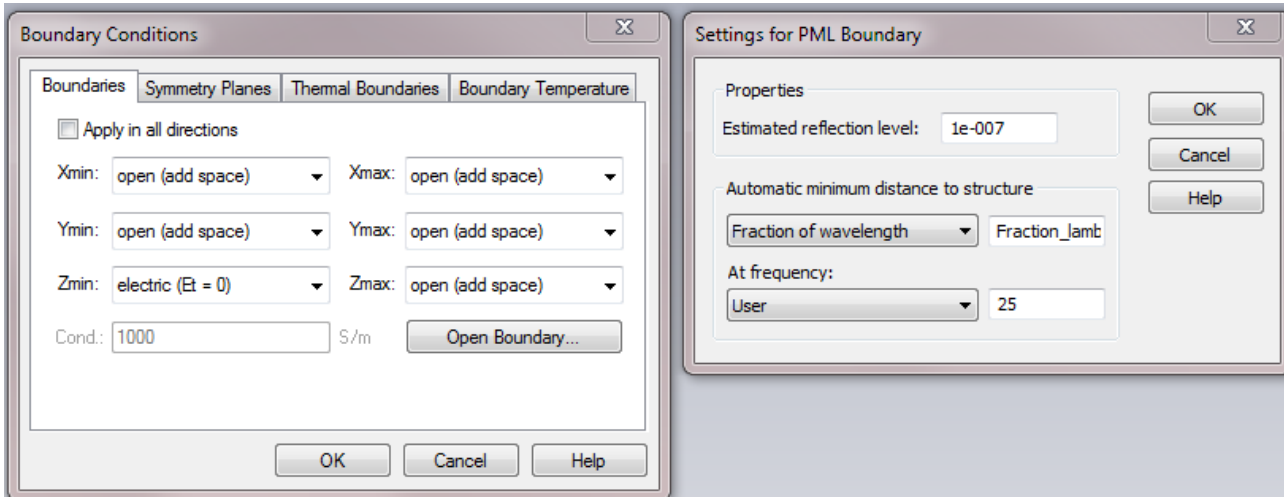


Figure 9. The Bounding Box menu and the Open Boundary sub-menu.

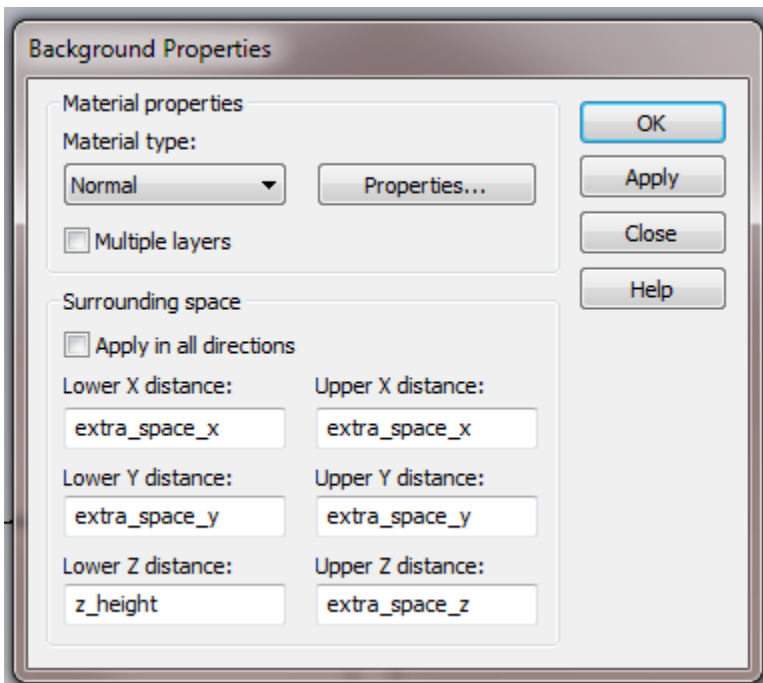


Figure 10. The Background menu. Extra simulation space can be added to the simulation, but it is not clear how to add space and improve the simulation at this point. Again, 25 MHz was not a typical frequency for extra space calculations. 50-75 MHz numbers yielded better results.

Table 1 below lists the parameter settings found to be most useful for getting good results. Mesh line limit ratio should be used instead of minimum cell size as the latter caused meshing problems for reasons unknown.

Parameter Name	Value	Description
Frequency Range of Interest	100 – 190 MHz	
Frequency Range of Simulation	50 to 250 MHz	
Hexahedral Legacy Grid	Selected	Alternative is the 2014 version
Solver Accuracy	-80 dB	Highest setting
Solver Specials	Number of pulses = 50	
EFPBA Solver	Selected	
Mesh Lines per wavelength	110	Beginning Value for adaptive mesh runs. 150 found to be a good value.
Max to min ratio	50	Might not be used correctly in mesh, but do not specify minimum cell size as this setting can cause problems.
Sub-gridding	Enabled	
Point Accuracy Enhancement	90%	Lower values might be OK
Adaptive Meshing	Energy Method	Sub-gridding turned off
	Adapt in x, y, and z directions	
	0.7 Mesh growth	
	4 passes min 7 maximum	Adjust as needed
	Delta S11 = 0.001	
	frequency range = 80 to 200 MHz	Range of interest
Bounding Box	Add 1/8 wavelength at 50 MHz	75 MHz was also used
	Reflection estimate 1e-7	Reflection off boundaries
Background extra space	Added 30" in x extra sim space	Perpendicular to thin wire
	Added 15" in z extra sim space	Amount above the ground plane
	No extra sim space in y	Y is along the excitation axis
	(try without extra space anywhere)	

Table 1. Settings recommended for the finite length dipole over a ground plane evaluated over the frequency range of 100 to 190 MHz. Adding additional space seems to generally make the results worse. This might be countered by increasing the mesh count, but higher mesh counts tended to decrease the quality of the results once a certain threshold was reached. Try the simulation without adding extra space.

II. Finite Horizontal Dipole over a Ground Plane Results

Results from simulation experiments with the horizon dipole. Part 2.

A. Introduction

This report is the follow up study to the previous report, “*Finite Length Horizontal Dipole over a Ground Plane Theory vs Simulation*,” (Nov 11, 2014) which showed problems at the low end of the frequency range. That report called for a follow up study to improve CST accuracy. This study holds the dipole physical features constant (except for run #2 where the gap was changed from 0.05” to 0.50”) and focuses on the meshing and accuracy parameters. The simulation parameters of the previous study are listed in Tables A1 and A2. Typical results of the previous study, showing the issues with the convolution results, are shown in Figures A1-A5 and Figures 60-67.

The simulation dipole studied is a $\frac{1}{2} \lambda$ (176.7 MHz) horizontal dipole of total length 33.42” placed 16.71” ($\frac{1}{4} \lambda$) above a ground plane. It is compared against a theoretical infinitely thin dipole for which an analytical solution to the beam pattern is known. The simulation wire has a finite diameter of 0.05” and a center feed gap of 0.05” which departs from the ideal dipole of infinitely thin and no gap. Figure 11 shows the gap, and Figures 12 and 13 show the meshing of the gap with and without sub-gridding which was explained in the first half of this report.

The design wavelength was chosen to be 176.7 MHz to replicate the EDGES antenna. Typical beam patterns can be seen in Figs. 14 -15. The metric used to judge the results is the RMS error obtained by fitting a 4th order polynomial in log frequency to the dipole antenna’s response to the sky which is formed by convolving the antenna beam with a Haslam 408 MHz sky map, scaled to other frequencies using an index of -2.5.

38 simulation runs (see Table 2.) were made varying the meshing and accuracy parameters. The remainder of this report will discuss the results and learnings from these simulations.

B. Method

The previous study used PBA meshing with 75 mesh lines per wavelength with the highest wavelength set to 220 MHz and set the S11 accuracy to -50dB. (see Table A1). This study explores the realm of higher mesh lines (~150), which requires FPBA with Enhanced accuracy, higher top frequency settings 250 MHz, and higher S11 accuracy (-80 dB).

Extra space was set to 1/8 (CST default setting), but calculated at a wavelength of 50 MHz, not 100 MHz as in the previous study. Extra space was varied, but again, too much extra space was found to be very detrimental to the results.

Sub-gridding is also explored as well as both of the adaptive mesh methods – Expert system based and Energy system based. Table 2 describes the simulation settings used in this study. The variations selected are by no means exhaustive and it is possible that there is a key parameter that has been overlooked. The most influential parameter settings appear to be a dense, but not over dense mesh, a higher top frequency setting (which also affects mesh density), and not an overabundance of extra simulation space.

Three sets of variations, runs 29-38, used the new 2014 meshing system. The results using the new system were similar to those of the old system, although the new system was not explored in the same detail as the previous meshing system. The results section will discuss the findings from the 38 simulation runs.

C. Results

As mentioned earlier, the metric used to determine the goodness of a simulation is the RMS error resulting from a 4th order polynomial fit in log frequency to the antenna’s response to a frequency scaled Haslam sky map. As an example, results from Run #1 are compared against results from the analytical model in Figures 16 - 21. Results with CST derived beams for 2nd and 3rd order fits at the low RMS error location are very close to the theoretical results. Even the 4th order result is only a factor of 2 off, but the even lower RMS error values of 5th order and above achieved with the analytical beam are difficult to achieve with the CST derived beam. The high RMS error region tells the same story, but the CST

results match for 3rd and 4th order and begin to lag only at the 5th order. However, a 0.6 mK RMS error is a vast improvement over the results obtained with the previous meshing scheme which could not get below 2 mK of RMS error.

Short Dipole

One more data point that is not listed in the table of variations, but gives us hope for CST accuracy, is the infinitesimal length diode. The short thin analytical dipole over a ground plane has less structure than the finite length dipole because the beam is not dependent upon the length of the dipole, and CST actually does quite a fine job matching the analytical results. Figures 22-27 show that CST handles this case very well.

Energy Based Adaptive Meshing and S11 Convergence

Runs 14-17 used an Energy based adaptive mesh (see Table 1). Figure 28 shows the S11 response for the 4 passes. The simulation converges on an S11 pattern at the second pass. Figure 29 shows the convergence for an Expert based system using the 2014 meshing system. The two simulations converge to S11 patterns with minimums slightly different from each other, 163.55 MHz vs 163.10 MHz. The same minimum point is not always reached with different meshes (see Table 1).

RMS Error vs Run Number

The fourth order RMS error is plotted vs run number for the worst and best LST values at latitude -26 in Figures 30-33. As can be seen, 4th order results ranged between 0.5 mK and 2.2 mK for the low LST region, and 20 mK and 100 mK for the high LST region. Contrary to the favorable LST case, the least favorable LST case does see a decrease in RMS error when the order of the polynomial is increased from 4th order to 5th order. Eight runs were able to achieve sub mK error levels.

The results from the previous study are included Figures 34-35 to show that the results in this study were an improvement over the results of the previous study in which 5-10 mK RMS error values were the most common.

Derivative Plots Reveal Beam Structure

As we saw in Figures 16-21, the simulated finite dipole beam results are very close to the analytical results, but not quite as good. To determine the beam feature that is causing the deviation, we looked at the changes of the beam with frequency. Figures 36 – 43 show the derivative of the beams wrt frequency plotted as a frequency vs theta pcolor plot for both CST Run 15 and the analytical beam. The analytical beam changes very smoothly and evenly with frequency while the CST beam shows some speckling.

A slice through the pcolor plots at theta = 40 degrees is plotted to highlight additional structure that might give rise to the need for higher order polynomials. There is some jaggedness in these plots, but these are not an issue as the short dipole plots in figures 44-51 have this feature too, yet polynomials fit these curves very well (recall figures 22-27).

Run #10 is an example of a run that had less than ideal simulation parameters and shows higher RMS errors, Figures 52-59 show non-linearity features in the theta cuts. The derivative plots also look slightly distorted visually as can be seen when compared to the analytical results. Run 10 began with a relatively low mesh per wavelength setting of 110 mesh cells per wavelength and used a feature that may not be working quite right in CST – setting the minimum mesh step instead of setting the max/min ratio. For this reason, it is not recommended to use this mesh parameter option.

The derivative plots from the previous study, as mentioned before, are shown in Figures 60-67 where the serious problems at low frequencies can be easily seen.

D. Conclusions and Recommendations

From the results of this study, it is clear that an optimum mesh is needed to yield accurate results. The mesh should be as dense as possible, but not overly dense to the point of reducing accuracy. Adaptive meshing should be used, especially in the beginning, to find this point. The highest simulation frequency should be set above the desired frequency to make the simulator deal with finer structures. The same could be said about the low end, but it is not clear if this has an effect. Extra simulations space should be kept to a minimum, and only increased slowly while monitoring the results carefully. A certain amount of experimentation is needed in the beginning of a new project to determine appropriate mesh settings.

Previous Study Simulation Parameter Tables

Parameter	Value
Mesh Type	PBA
Lines per Wavelength	75
Lower Mesh Limit	45
Mesh Ratio Limit	65
Solver Accuracy	-50 dB
Edge Enhancement	85%
Frequency Range of Simulation	80 to 220 MHz
Frequency to Calculate Extra Space	100 MHz
Reflection at Boundaries	1×10^{-4}

Table A1. Common Simulation Parameters of the Previous Study.

Simulation Number	Simulation Boundary Distance to Structure (λ fraction)	Wire Diameter (inches)	Center Gap (inches)
1	1/1	0.05	0.50
2	1/1	0.10	0.50
3	1/2	0.05	0.50
4	1/2	0.10	0.50
5	1/4	0.05	0.50
6	1/4	0.10	0.50
7	1/8	0.05	0.50
8	1/8	0.10	0.50
9	1/16	0.05	0.50
10	1/16	0.10	0.50
11	1/32	0.010	0.010
12	1/32	0.010	0.50
13	1/32	0.025	0.025
14	1/32	0.025	0.500
15	1/32	0.050	0.025
16	1/32	0.050	0.050
17	1/32	0.050	0.100
18	1/32	0.050	0.250
19	1/32	0.050	0.500
20	1/32	0.050	0.750
21	1/32	0.10	0.50

Table A2. Description of the parameter settings for the previous study's CST runs.

Previous Study

CST Dipole, Lat = -26, 100-190 MHz fit.
Run 19: Added simulation space = $\lambda/32$,
Wire diameter = 0.05", gap = 0.50".

Analytical Dipole, Lat = -26, 100-190 MHz fit.

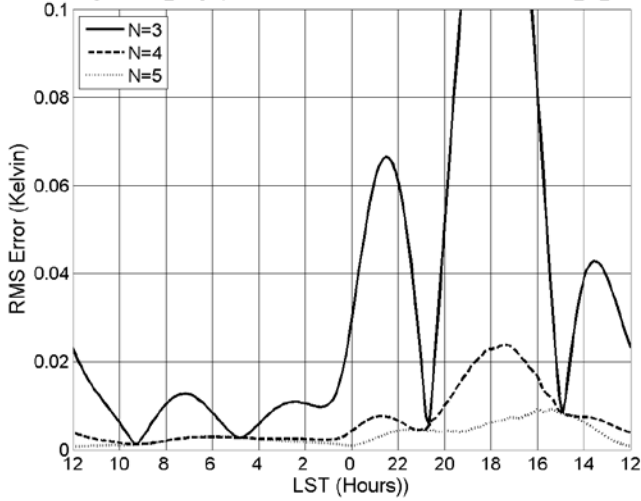


Figure A1. RMS Error vs LST.

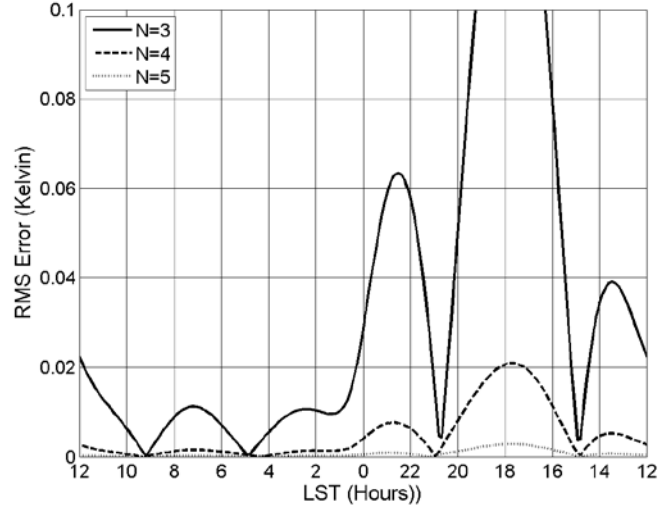


Figure A2. RMS Error vs LST.

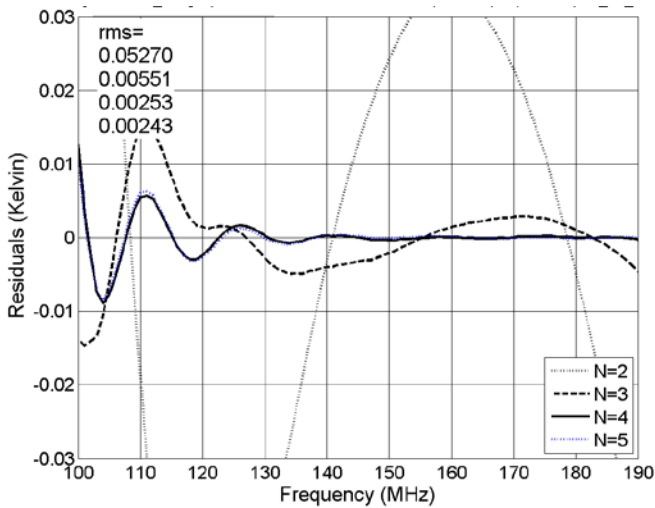


Figure A3. Residuals vs frequency, LST = 4.0 hrs.

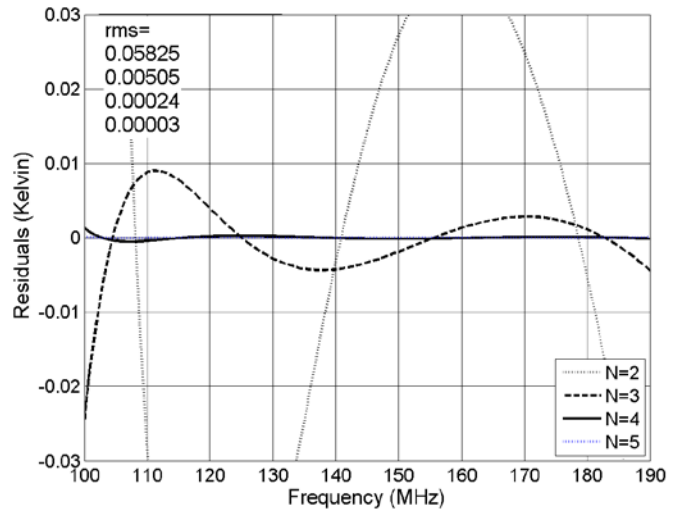


Figure A4. Residuals vs frequency, LST = 4.0 hrs.

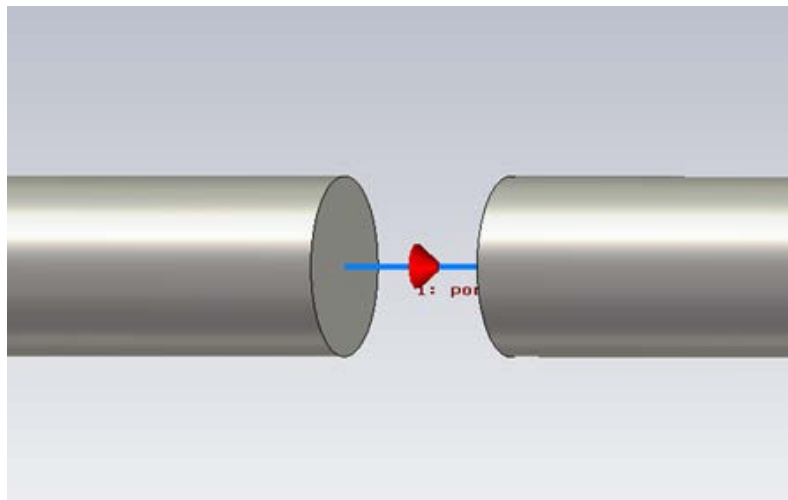


Figure 11. Gap section of the wire. Gap nominal distance = 0.05".

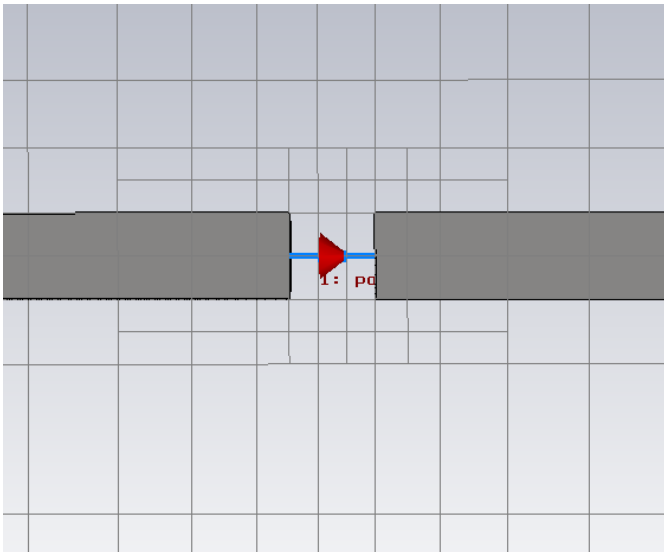


Figure 12. Meshing near the gap with sub-gridding.

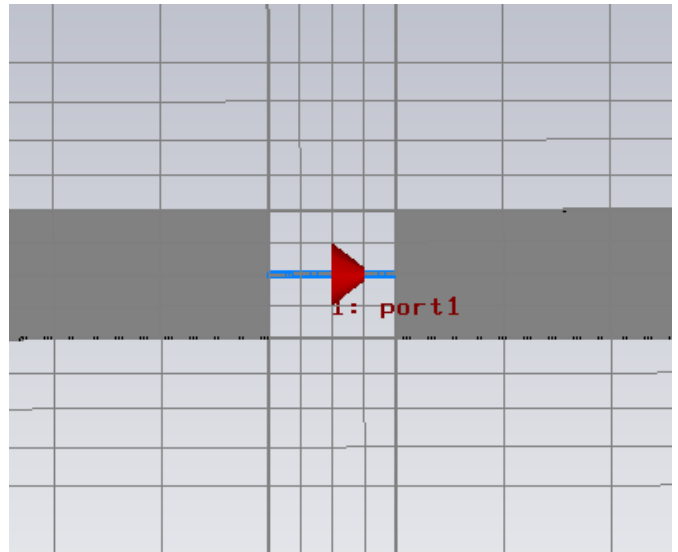


Figure 13 Meshing without sub-gridding.

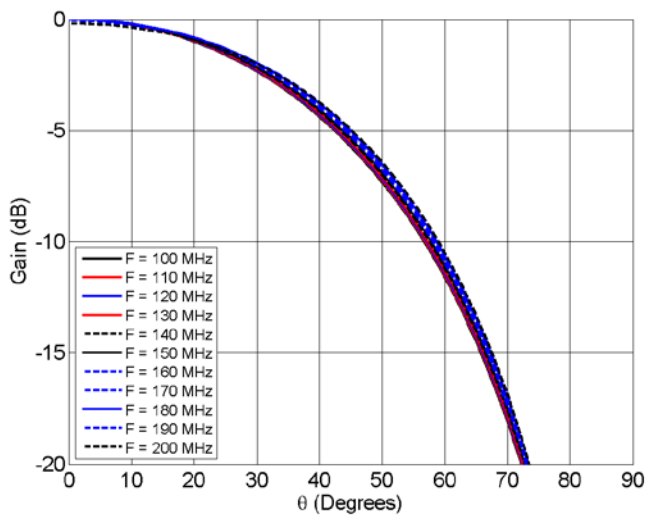


Figure 14. Typical beam pattern vs frequency for phi=0.

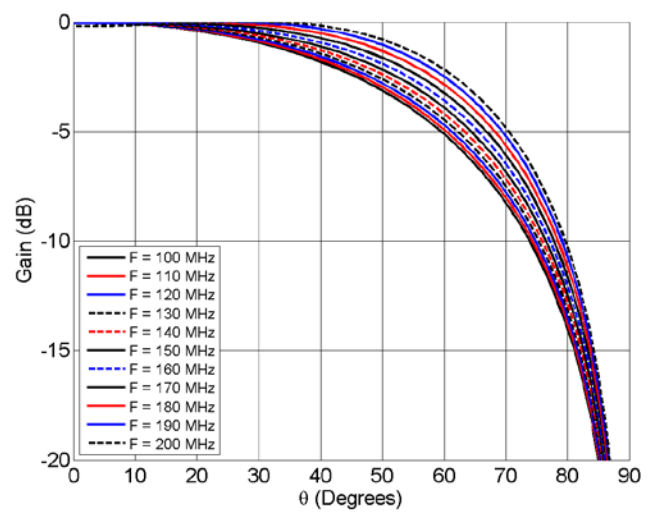


Figure 15. Typical beam pattern vs frequency for phi=90.

CST derived beam: "Finite Length Dipole", Run #1.
Lat = -26° Fit frequency range 100-190 MHz

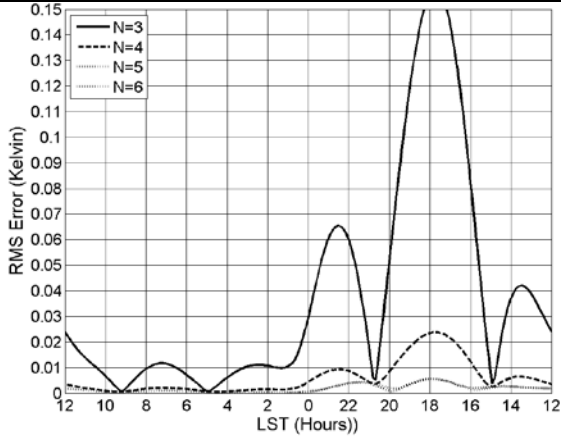


Figure 16. RMS Error vs LST for 3rd - 6th order log polynomial. Notice how the choice of LST becomes less critical as the order of the polynomial increases.

Analytical model beam: "Finite Length Dipole".
Lat = -26. Fit frequency range 100-190 MHz

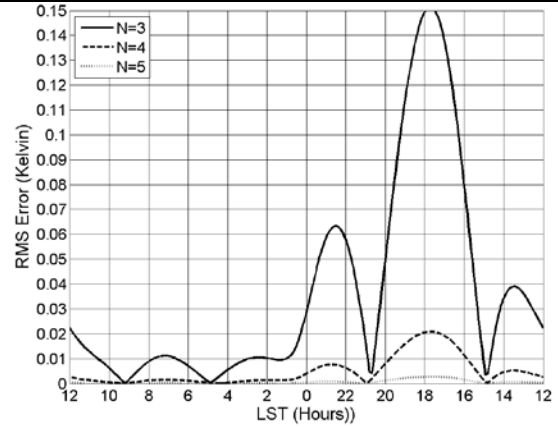


Figure 17. RMS Error vs LST for 3rd - 6th order log polynomial. Notice how a 5th order polynomial reduces the RMS error across the entire range of LST values.

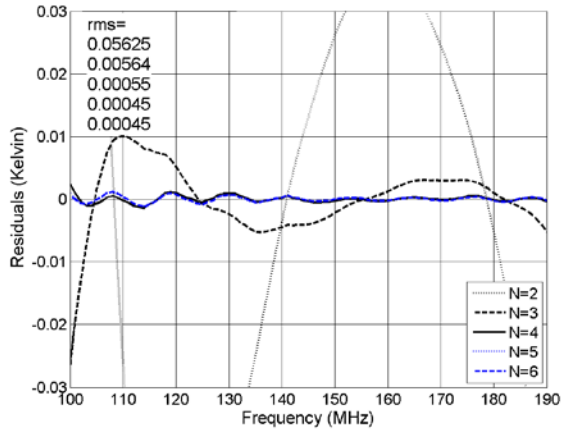


Figure 18. Residuals for a low RMS error region, LST = 4.0 hrs. Improvement saturates at N=4.

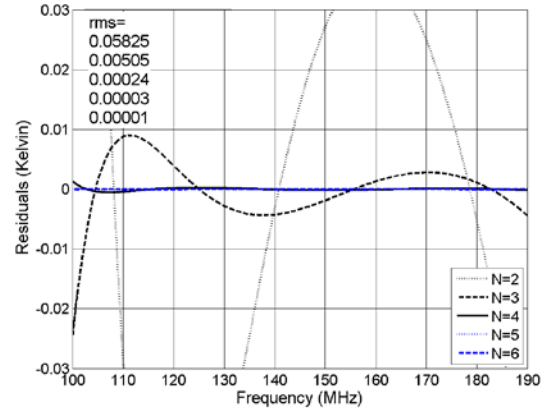


Figure 19. Residuals for a low RMS error region, LST = 4.0 hrs. Residuals improve with higher order.

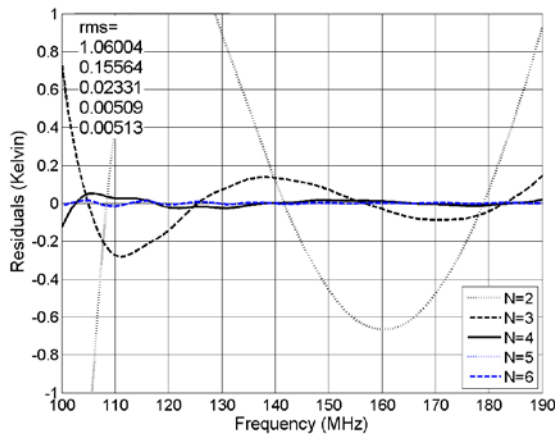


Figure 20. Residuals for a high RMS error region, LST = 17.3 hrs. Improvement saturates at N=5.

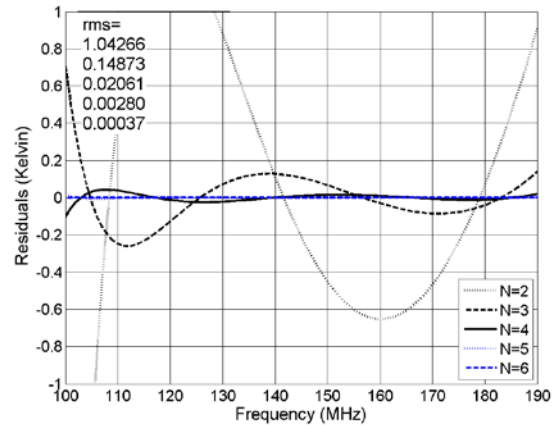


Figure 21. Residuals for a high RMS error region, LST = 17.3 hrs. Residuals improve with higher order.

CST derived beam: "Small Dipole", Lat = -26° Fit frequency range 100-190 MHz

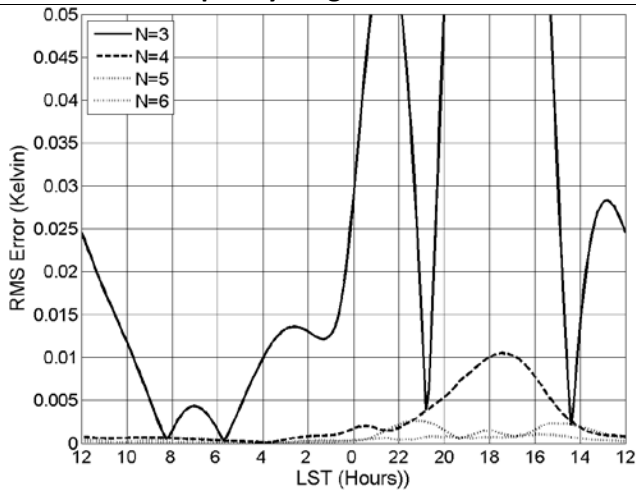


Figure 22. RMS Error vs LST for 3rd - 6th order log polynomial. Notice how the choice of LST becomes less critical as the order of the polynomial increases.

Analytical model beam: "Infinitesimal Dipole". Lat = -26. Fit frequency range 100-190 MHz

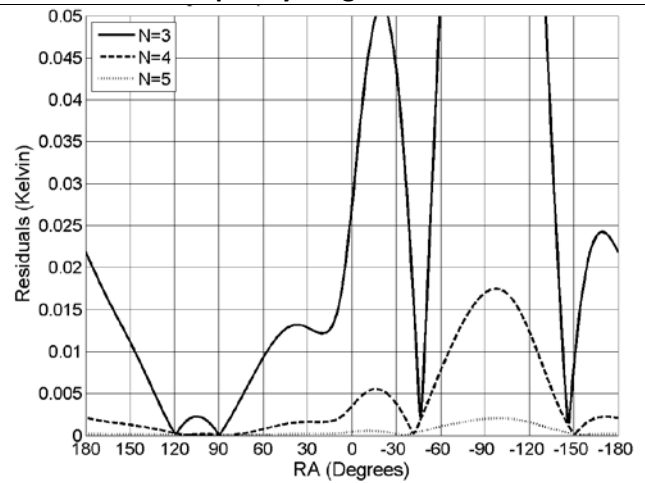


Figure 23. RMS Error vs LST for 3rd - 5th order log polynomial. Notice how a 5th order polynomial reduces the RMS error across the entire range of LST values.

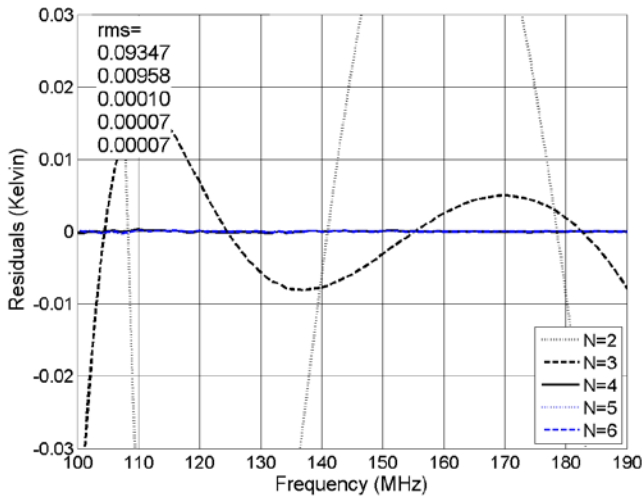


Figure 24. Residuals for a low RMS error region, LST = 4.0 hrs. Improvement saturates at N=4.

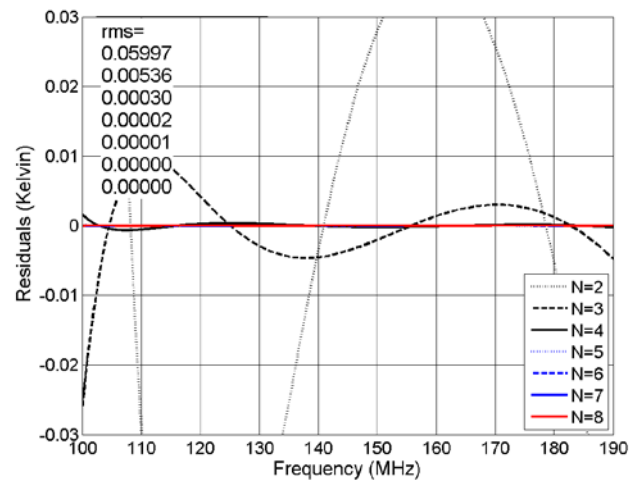


Figure 25. Residuals for a low RMS error region, LST = 4.0 hrs. Residuals improve with higher order.

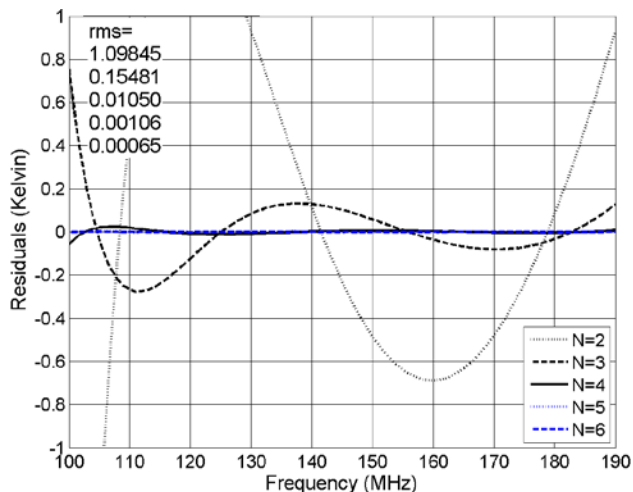


Figure 26. Residuals for a high RMS error region, LST = 17.3 hrs. Improvement saturates at N=5.

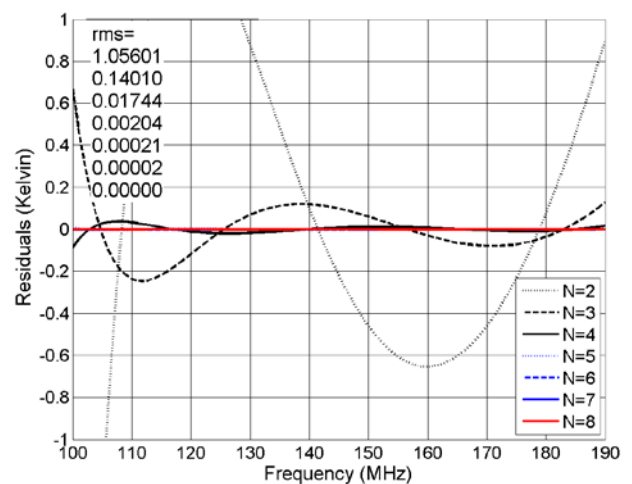


Figure 27. Residuals for a high RMS error region, LST = 17.3 hrs. Residuals improve with higher order.

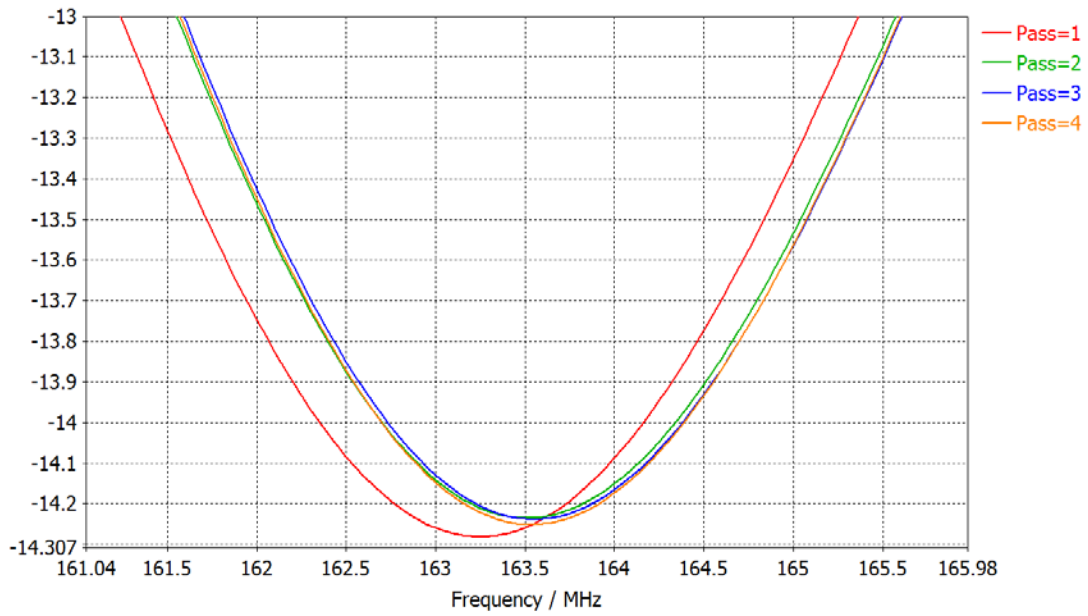


Figure 28. S11 for the 4 energy based adaptive mesh passes for CST runs 14-17. The minimum point converges to 163.55 MHz

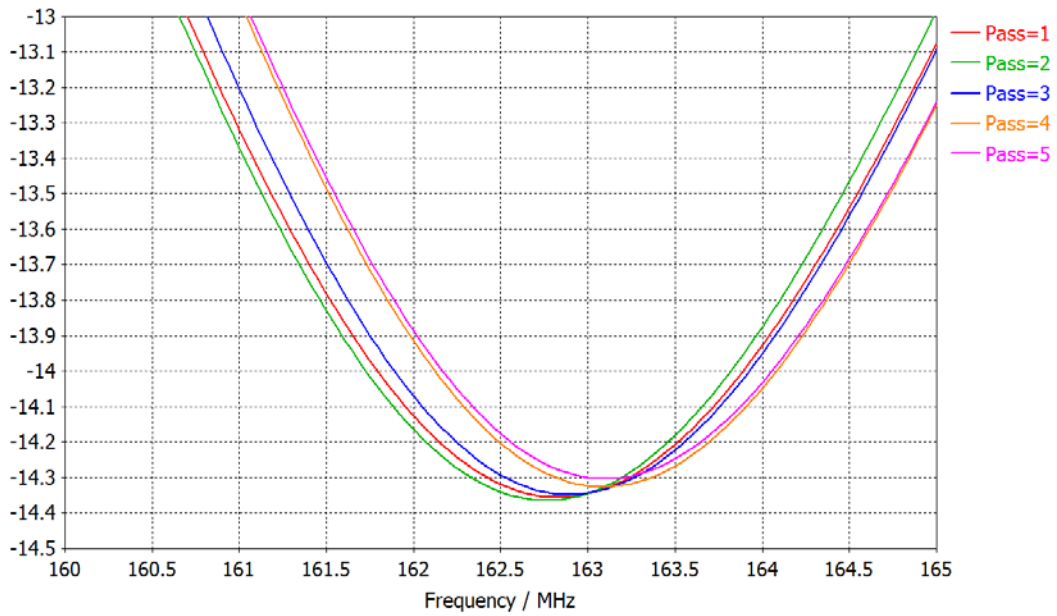


Figure 29. S11 for the 5 Expert based adaptive mesh passes for CST runs 18-23. The minimum point converges to 163.55 MHz.

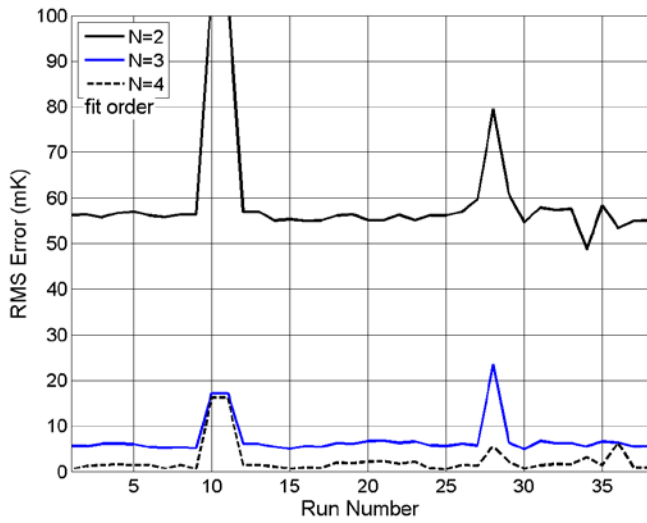


Figure 30. RMS Error vs CST Run number for the favorable LST location (4 hrs.), latitude -26.

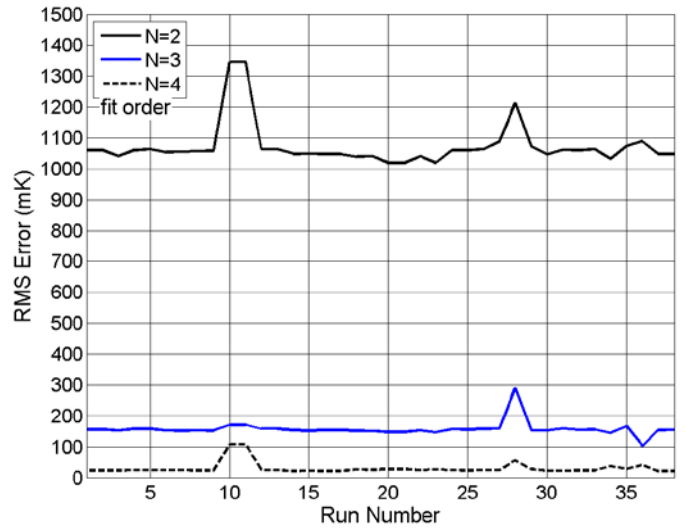


Figure 31. RMS Error vs CST Run number for the less favorable LST location (17.3 hrs.), latitude -26.

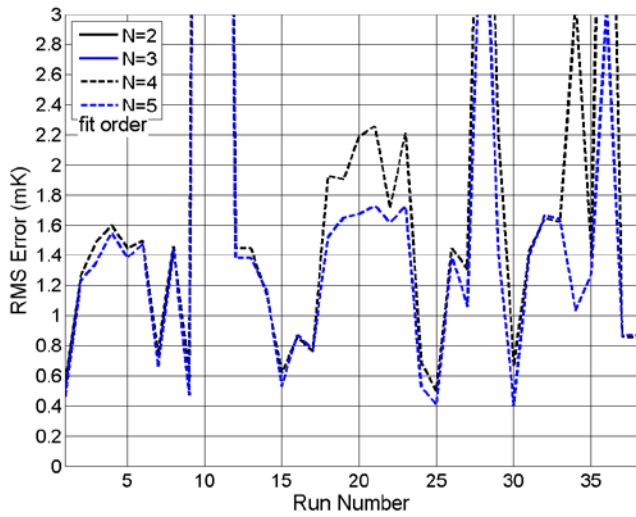


Figure 32. A closer look at Fig 30 and 5th order results added.

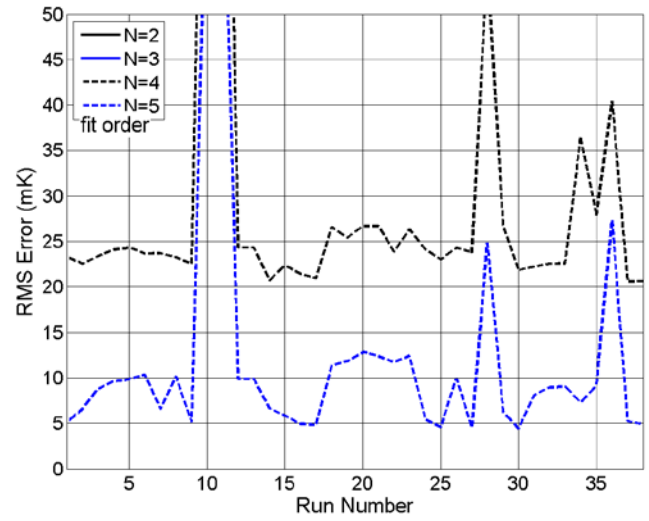


Figure 33. A closer look at Fig 31 with 5th order results added.

Previous Study – RMS Error vs. Run

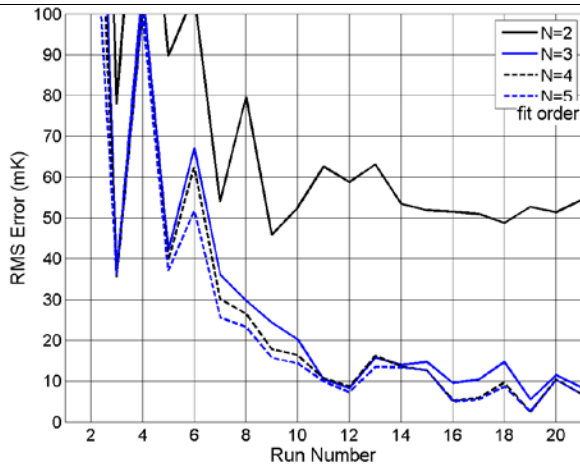


Figure 34. Previous Study, favorable LST location.

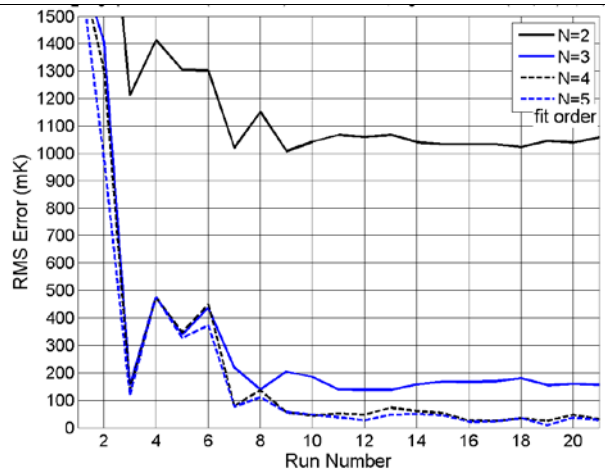


Figure 35. Previous study, unfavorable LST location.

Beam from CST Run #15 – Good Results

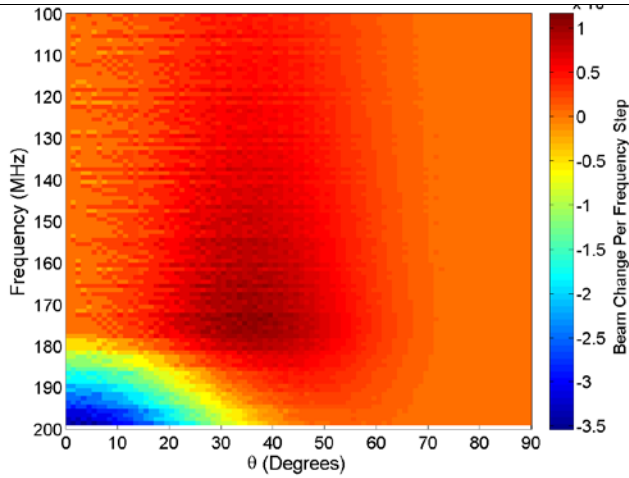


Figure 36. Derivative plot for $\phi = 0^\circ$.

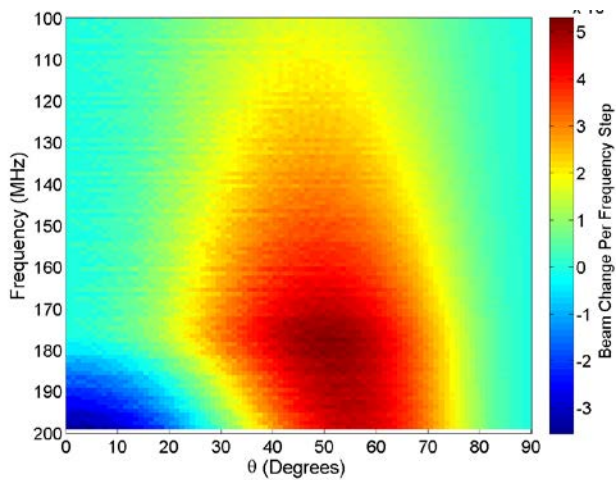


Figure 38. Derivative plot for $\phi = 90^\circ$.

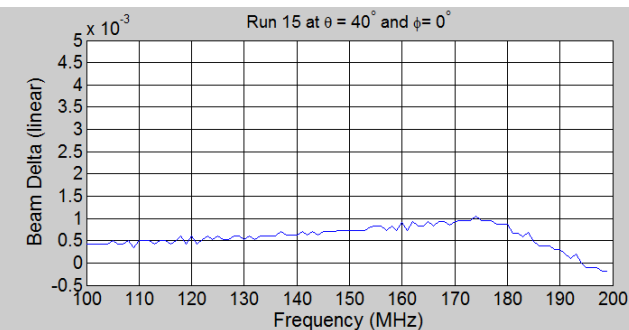


Figure 40. Cut through $\theta = 40^\circ$, $\phi = 0^\circ$.

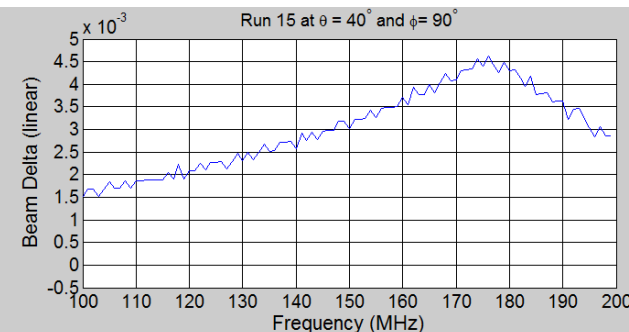


Figure 42. Cut through $\theta = 40^\circ$, $\phi = 90^\circ$.

Analytical Beam

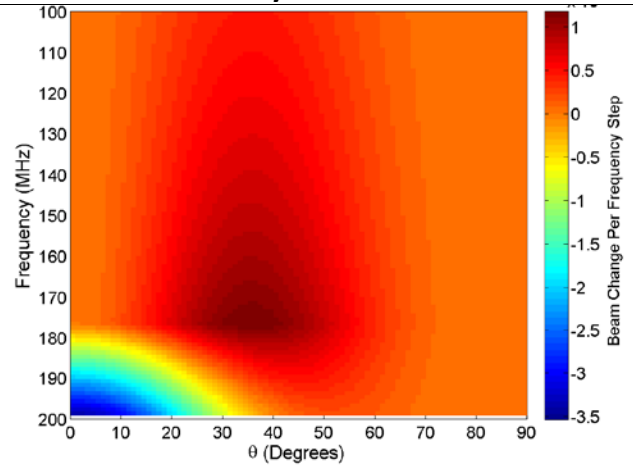


Figure 37. Derivative plot for $\phi = 0^\circ$.

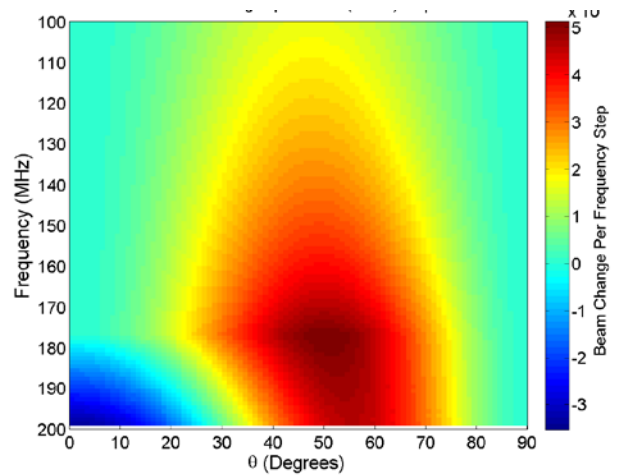


Figure 39. Derivative plot for $\phi = 90^\circ$.

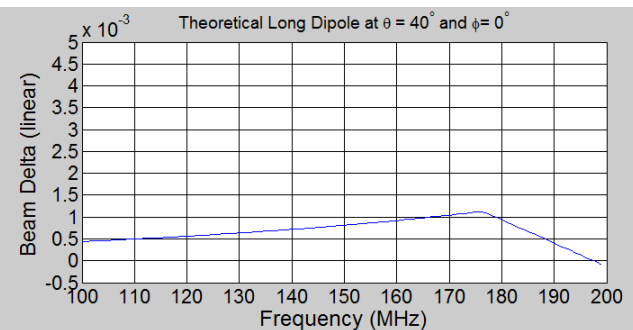


Figure 41. Cut through $\theta = 40^\circ$, $\phi = 0^\circ$.

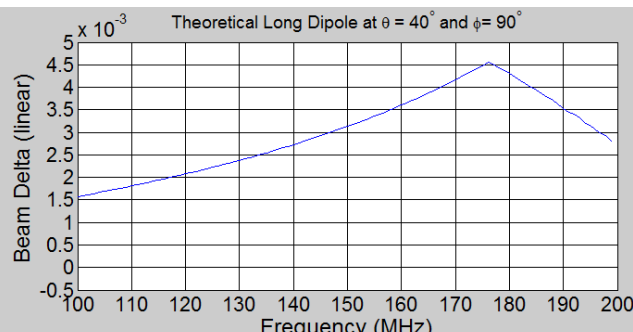


Figure 43. Cut through $\theta = 40^\circ$, $\phi = 90^\circ$.

Small Dipole Beam from CST

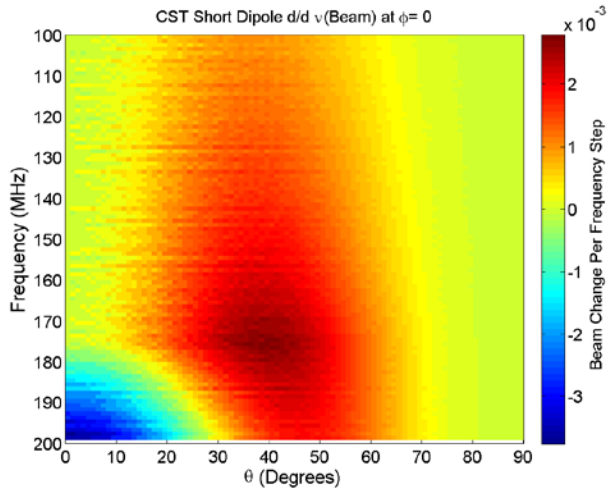


Figure 44. Derivative plot for $\phi = 0^\circ$

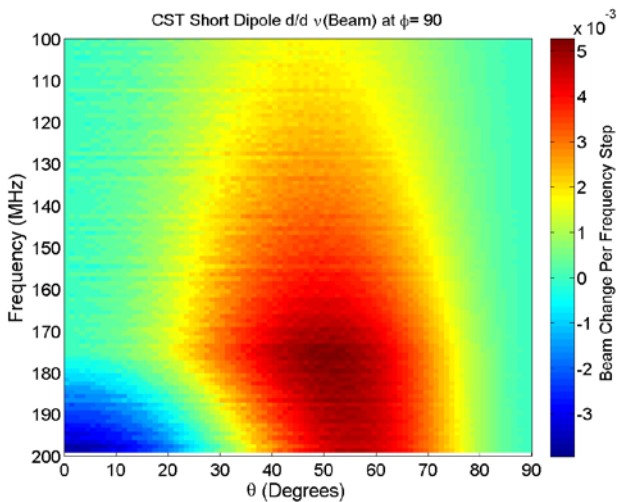


Figure 46. Derivative plot for $\phi = 90^\circ$

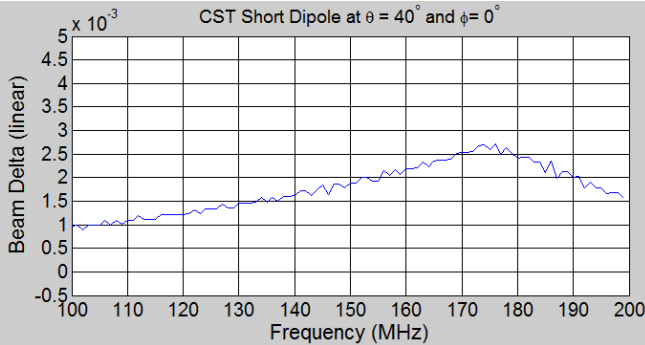


Figure 48. $\phi = 0^\circ$, $\theta = 40^\circ$ cut line

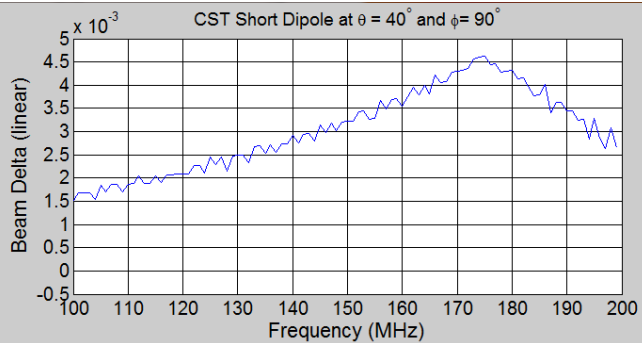


Figure 50. $\phi = 90^\circ$, $\theta = 40^\circ$ cut line

Analytical Small Dipole Beam

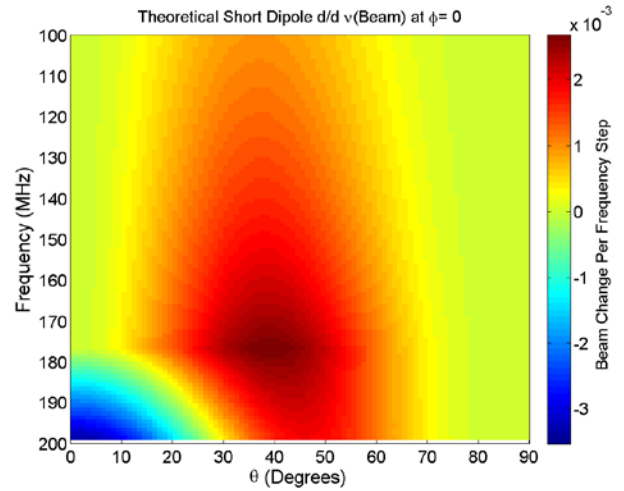


Figure 45. Derivative plot for $\phi = 0^\circ$

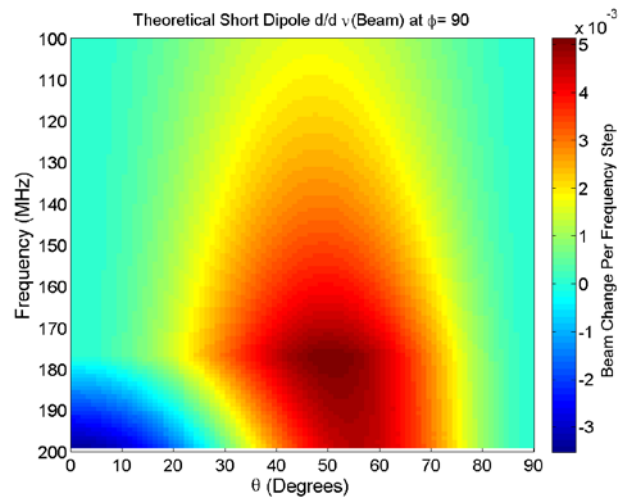


Figure 47. Deriv. plot for $\phi = 90^\circ$

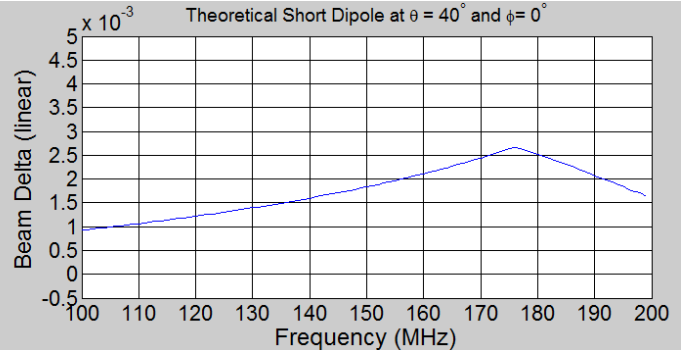


Figure 49. $\phi = 0^\circ$, $\theta = 40^\circ$ cut line

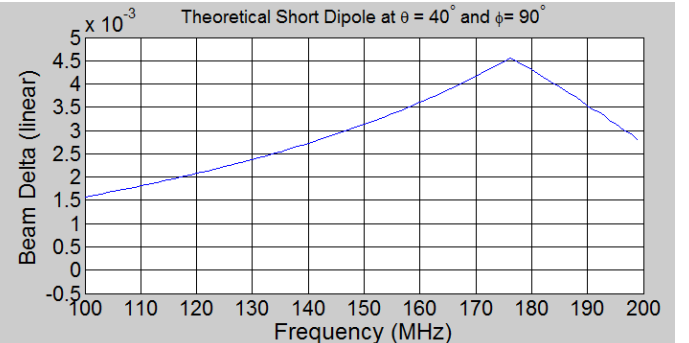


Figure 51. $\phi = 90^\circ$, $\theta = 40^\circ$ cut line

CST Run #10 – High RMS Run

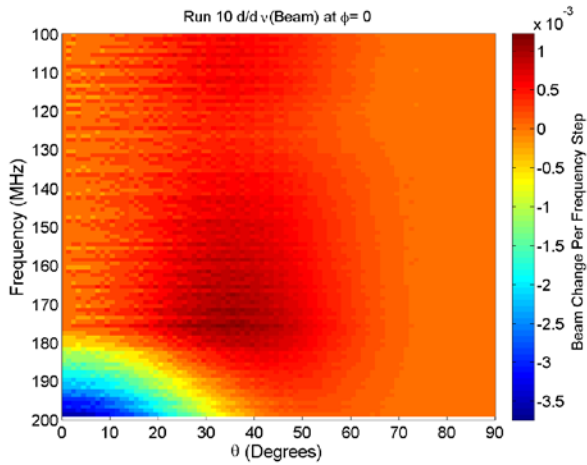


Figure 52. Derivative plot for $\phi = 0^\circ$.

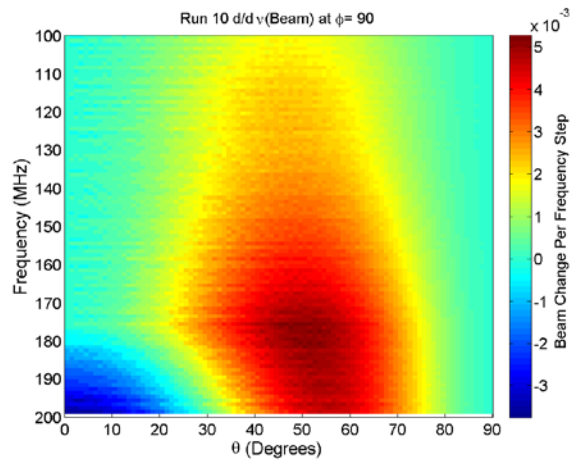


Figure 54. Derivative plot for $\phi = 90^\circ$.

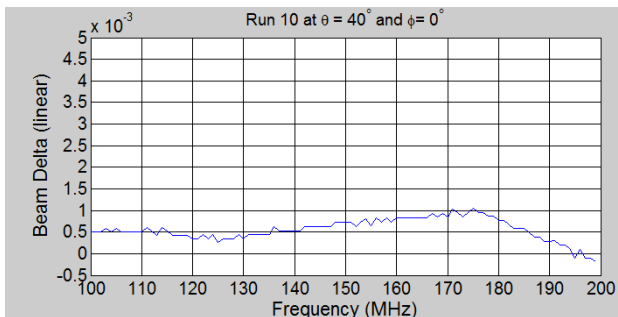


Figure 56. $\phi = 0^\circ$, $\theta = 40^\circ$ cut line.

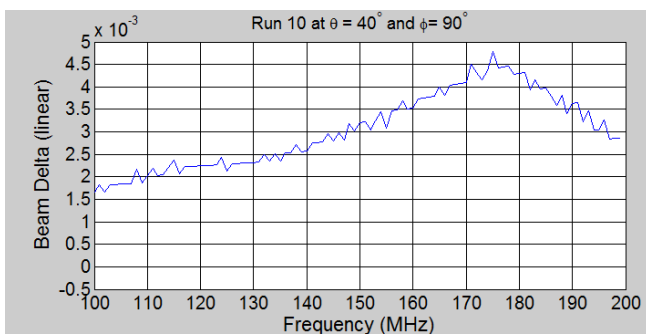


Figure 58. $\phi = 90^\circ$, $\theta = 40^\circ$ cut line.

Analytical Beam

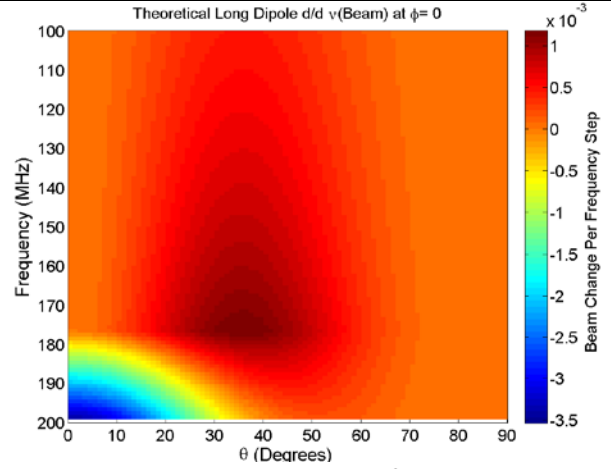


Figure 53. Derivative plot for $\phi = 0^\circ$.

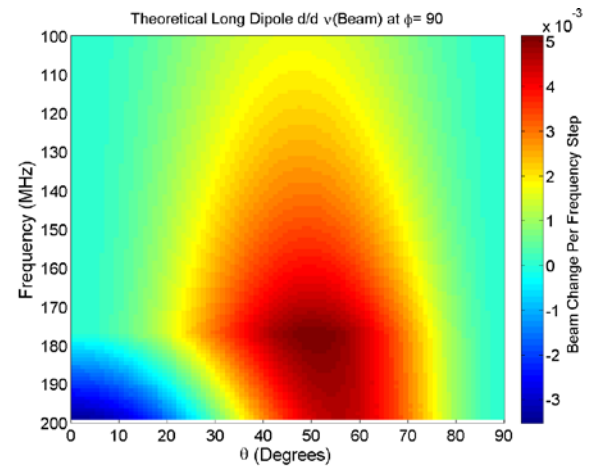


Figure 55. Derivative plot for $\phi = 90^\circ$.

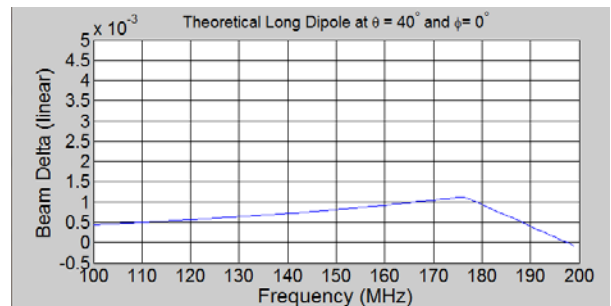


Figure 57. $\phi = 0^\circ$, $\theta = 40^\circ$ cut line.

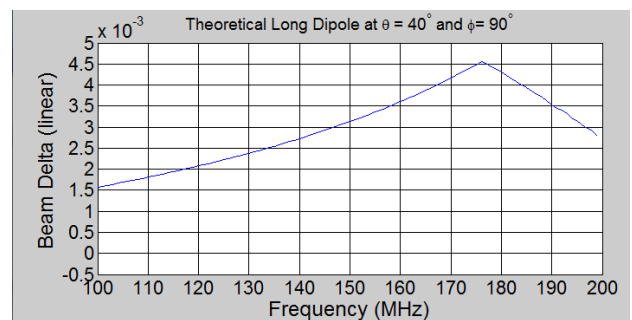


Figure 59. $\phi = 90^\circ$, $\theta = 40^\circ$ cut line.

Previous Study – Defects in the Beam are Evident

CST Beam Run 19 (see Table A1)

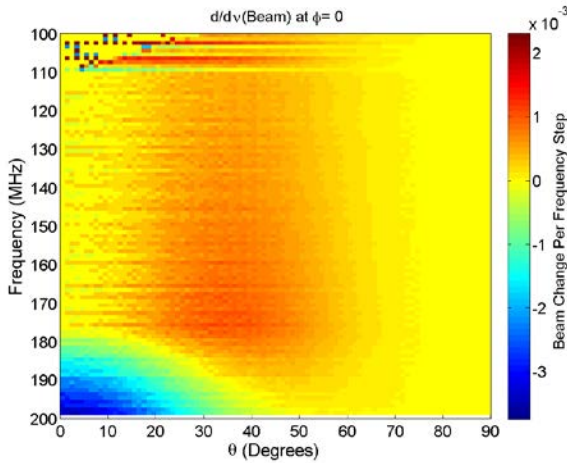


Figure 60. Derivative plot for $\phi = 0^\circ$.

CST Beam, Run 7 (see Table A1)

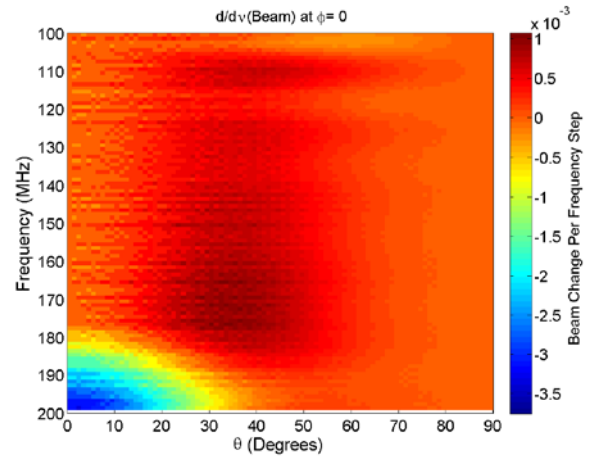


Figure 61. Derivative plot for $\phi = 0^\circ$.

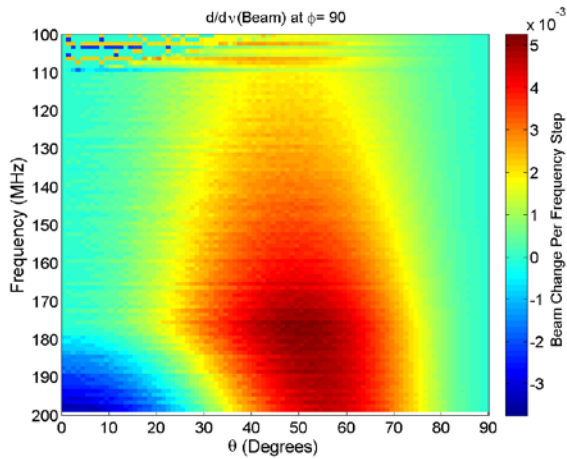


Figure 62. Derivative plot for $\phi = 90^\circ$.

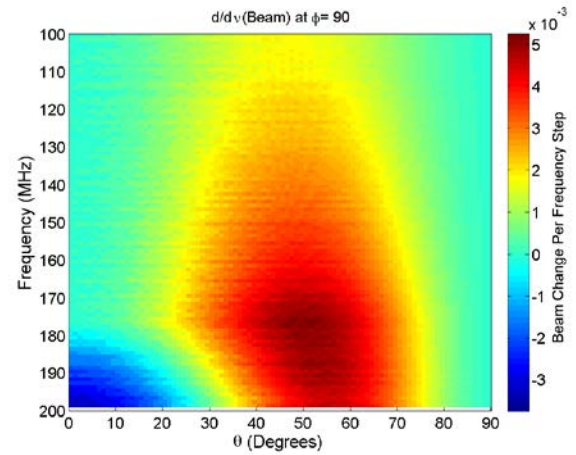


Figure 63. Derivative plot for $\phi = 90^\circ$.

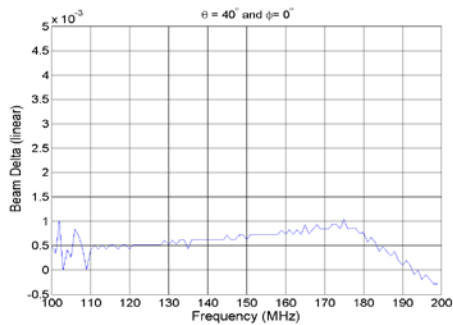


Figure 64. $\phi = 0^\circ$, $\theta = 40^\circ$ cut line.

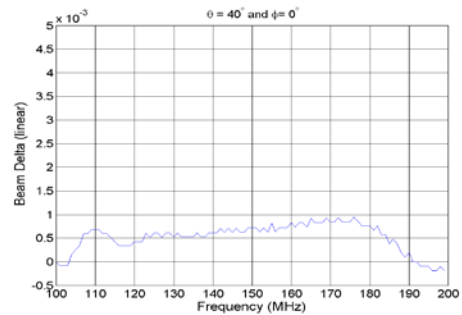


Figure 65. $\phi = 0^\circ$, $\theta = 40^\circ$ cutline.

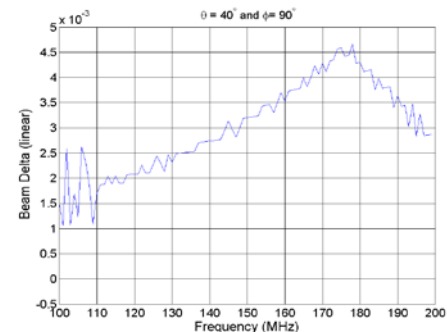


Figure 66. $\phi = 90^\circ$, $\theta = 40^\circ$ cut line.

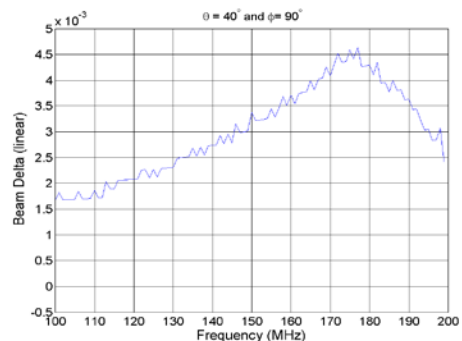


Figure 67. $\phi = 90^\circ$, $\theta = 40^\circ$ cut line.